

Contents lists available at ScienceDirect

Journal of Membrane Science

journal homepage: www.elsevier.com/locate/memsci



Preparation of isoporous membranes from low χ block copolymers via coassembly with H-bond interacting homopolymers



Guo-Dong Zhu^a, Cao-Ying Yang^a, Yu-Rong Yin^a, Zhuan Yi^{a,b,*}, Xian-Hong Chen^{a,b}, Li-Fen Liu^{a,b}, Cong-Jie Gao^{a,b}

- ^a Department of Ocean, Zhejiang University of Technology, Hangzhou, 310014, China
- b Huzhou Institute of Collaborative Innovation Center for Membrane Separation and Water Treatment, 1366 Hong Feng Road, Huzhou, 313000, China

ARTICLE INFO

Keywords: Isoporous membranes Co-assembly Block copolymers SNIPS PNIPAM

ABSTRACT

Self-assembly and non-solvent induced phase separation (SNIPS) was extensively used in the fabrication of isoporous membranes for its compatibility with massive production. However, for the well-defined SNIPS, preparation of isoporous membranes from low χ block copolymers is challenging because self-assembly of these polymers is usually hard to induce. In this work, we showed that such a problem could be effectively overcome through the co-assembly strategy by blending with homopolymers that interacted with block copolymers (BCPs). For the polystyrene-block-poly(N-isopropylacrylamide) (PS-b-PNIPAM) which has relatively small Flory-Huggins interaction parameter ($\chi \approx 0.05$), the formation of the isopores was readily induced when polyacrylic acid (PAA) was added as an additive. Three PS-b-PNIPAM with the PNIPAM mass fractions ranging from 5.9 to 36.5 wt% were used as membrane-forming materials, and three PAA with different molecular weights (MWs) were used to investigate how MWs of homopolymer affected the isopore formation. The selective H-bonding of PAA with PNIPAM was in-situ determined by infrared spectroscopy, which was further supported by the small angle X-ray scattering that indicated the microphase separation of PS-b-PNIPAM in solution was remarkably enhanced by PAA. The contribution of PAA on isopore formation was also found for the casting solutions of a wide range of concentrations and different solvent compositions. Our finding showed herein actually provided a facile route to prepare isoporous membranes from low χ BCPs under general conditions.

1. Introduction

Membrane separation has played increasingly important roles in modern chemical engineering because of its high efficiency and energy saving. The permeability, selectivity, and fouling-resistance are three critical aspects for membrane separation [1], and great effort had been devoted to improving both or all of them in past years. One of the methods that will simultaneously increase the selectivity and permeability is the preparation of isoporous membranes. Typically, isoporous organic or inorganic membranes can be fabricated through anodization, templating, track etching, micro-electromechanical systems (MEMS) and self-assembly of block copolymers (BCPs) [2-6]. However, compared with the others, self-assembly of BCPs has attracted more attention because the pore size and pore chemistry can be tailor-made with the precisely synthesized polymers [6]. Self-assembly and non-solvent induced phase separation (SNIPS) was a recently developed strategy that was used to fabricate isoporous membranes from self-assembling polymers [7]. Different from some other methods such as selective

etching, SNIPs is highly compatible with industrial fabrication, which allows the membranes to be produced in a fast, successive and large-scale manner [8]. In addition, isoporous membranes prepared from SNIPS are usually free-standing, which allows them to be used directly without transfer. Relatively speaking, SNIPS is a robust strategy that generates isoporous membranes in an effective and efficient way.

Typically, microphase separation is necessary for the generation of isoporous membranes from block copolymers [9]. This means that block polymers need to have sufficient segregation strength, which is a function of the Flory-Huggins parameter (χ_0) and the degree of polymerization (N), to induce the self-assembly. For the membranes prepared through SNIPS, microphase separation is required for the BCPs dissolved in solutions. However, the Flory-Huggins parameter between solvated polymer blocks is diluted by solvents, and the effective χ should be written as χ effective = χ_0 C, where the χ effective is the effective Flory-Huggins parameter in solution, and the C is the concentration of block copolymers [10]. For the typical SNIPS process, the C is usually in the range from 10–30 wt%, which means that χ effective is only 10–30%

^{*} Corresponding author. Department of Ocean, Zhejiang University of Technology, Hangzhou, 310014, China. *E-mail address*: zhuann.yi@gmail.com (Z. Yi).

of the χ_{0} found in bulk state. Therefore, to the successful fabrication of isoporous membranes through SNIPS, block copolymers must have larger N or higher χ_0 . Up to now, most of the isoporous membranes prepared by SNIPS were using PS-b-P4VP [7,11-13], which was known for its large χ value of around 0.35 [14,15]. Isoporous membranes were also successfully prepared from PS-b-PHEMA and PS-b-PAA that had the χ values of about 0.37 and 0.18, respectively [16,17]. Actually, block copolymers including the PS-b-P4VP, PS-b-PHEMA and PS-b-PAA were usually expressed as high χ polymers, because their χ values are several times to one order magnitude larger than normally found polymers such as PS-b-PMMA, PS-b-PI and others [16,18–20]. This interpretation reflects that polymers possess higher γ are preferred when isoporous membranes are fabricated via SNIPS. As another interesting polymer. PS-b-PEO gives the χ value of ~0.05 [21], which is only 1/7 to that of the PS-b-P4VP and PS-b-PHEMA. As a result, the membranes prepared from PS-b-PEO presented obviously inferior pore organization than that of the membranes prepared from PS-b-P4VP and PS-b-PHEMA. Since the molecular weights (N) of BCPs used for membrane formation is in the same order (100–200 kg/mol) [13,22,23], the much smaller χ and the resultant lower segregation strength (\(\chi\)N) is the major reason responsible for this inferior pore formation. A similar result is found for the recently developed block copolymer PS-b-PNIPAM ($\chi \approx 0.05$), which was successfully fabricated into isoporous membranes under a specifically designed solvent system. However, the prepared membranes gave a rather low permeability (~2 L/h·m²·bar), and the pore density, as well as the poor organization, was also obviously inferior to that found for membranes prepared from PS-b-P4VP. From the above expressions, we can find that the properties of block polymer are critical factors when SNIPS is used as the method to produce isoporous membranes.

Although BCPs with high χ values are preferred by the SNIPS, there are only limited high γ BCPs [24]. More importantly, lots of BCPs have fantastic functionalities for membrane application but they belong to low y polymers. For those BCPs, fabrication of isoporous membrane from them is challenging while also interesting. Theoretically, several ways can be adopted to strengthen the microphase separation for low χ BCPs in solutions. Firstly, increase the degree of polymerization (N). However, this strategy will lead to large pore size and will further prevent their applications from molecular separation [25,26]. Besides, from the aspect of polymerization, synthesis of BCPs with ultrahigh MWs is sometimes challenging and technique intensive. Secondly, increase the concentrations of BCPs in solution. However, this method will lead to an obvious increase in material consumption as well as the fabrication cost, causing additional problems for their practical applications. Therefore, a facile and effective method that can be used to fabricate isoporous membranes from those moderate or low χ BCPs is urgently required.

Recently, the functions of additives on tailoring the structures of isoporous membranes have been increasingly realized. Nunes found that the metal salt such as copper (II) acetate added to solutions had greatly improved the isoporous structures at non-optimized concentrations [27]. Less toxic salt such as magnesium acetate was also found to work effectively [28]. Besides, Abetz observed that molecules such as carbohydrates could be used as organic additives to improve membranes porosity and pore size distribution [29]. We recently found that organic acids added to solution increased the time window that retained isoporous structure [30]. These findings implied that the self-

assembly of BCPs could be facilitated by foreign additives. However, until now, additives used were only limited to small molecules [28–30], and the BCPs used for membrane preparation, typically, the PS-b-P4VP and PS-b-PHEMA, also belonged to high χ polymers. And thus far, the blending of macromolecular additives with BCPs of either high or low χ values has not been developed for SNIPS.

To successfully fabricate isoporous membranes from BCPs with small γ values, this work investigated the membrane formation from PS-b-PNIPAM through the co-assembly strategy, which used polyacrylic acid (PAA) as the macromolecular additive for PS-b-PNIPAM and membranes were prepared through well-defined SNIPS. PAA was known for its selective interaction with PNIPAM in aqueous solution [31,32], however, its contribution to self-assembly and isopores formation had never been studied in the SNIPS process. By using the small angle X-ray scattering (SAXS) analysis, we found that the phase separation of PS-b-PNIPAM in casting solution had been greatly improved. More importantly, as a result of increased microphase separation, our membranes fabricated from the co-assembly strategy showed obviously improved pore ordering and permeability (increased from 0.84 to 11.40 L/h·m²·bar). Finally, we also demonstrated that the coassembly strategy was applicable to casting solutions of a wide range of concentrations and solvent compositions, the phenomena of which was typically found for the higher χ BCPs before. In brief, this study had provided a facile while effective way to prepare isoporous membranes from low χ BCPs under very accessible conditions.

2. Experimental section

2.1. Material and reagents

Styrene was purchased from Energy Chemical, and inhibitors were removed by passing through the alkaline alumina column. N-isopropylacrylamide (NIPAM) was purchased from Energy Chemical and purified by recrystallization in hexane. Acrylic acid was purified by vacuum distillation. Adipic acid (AA), citric acid (CA), 1, 4-dioxane (DOX), tetrahydrofuran (THF), dimethylformamide (DMF), Acetonitrile (ACN) and other reagents were analytical purity and used as received.

2.2. Synthesis of the block copolymers

Polystyrene-block-poly(N-isopropylacrylamide) (PS-b-PNIPAM) copolymers were synthesized following a well-defined reversible addition-fragmentation chain transfer (RAFT) polymerization. The details for synthesis were showed in Supporting Information (S1.1). Three PS-b-PNIPAM with different compositions were obtained, which were described as PS_{520} -b-PNIPAM $_{139}$, PS_{430} -b-PNIPAM $_{227}$, and PS_{560} -b-PNIPAM $_{32}$, respectively. The subscripts represented the degree of polymerization for each block. The molecular weights, molecular weight distribution and compositions and were determined by GPC and NMR, respectively, and results were shown in Table 1.

2.3. Synthesis of PAA homopolymer

PAA with narrow molecular distribution was synthesized throw the RAFT polymerization. The detail for polymerization was shown in Supporting Information (S1.2). Three PAA with different degrees of polymerization (DPs) were obtained, which were described as PAA₃₅,

Table 1 Molecular characteristics of PS-*b*-PNIPAM copolymers.

Polymers	M _n (GPC) g/mol	M _w (GPC) g/mol	M _n (NMR) g/mol	PDI (GPC)	PNIPAM wt%
PS ₅₆₀ -b-PNIPAM ₃₂	40,712	57,146	61,849	1.39	5.9
PS ₅₂₀ -b-PNIPAM ₁₃₉	30,073	40,220	69,766	1.34	22.5
PS ₄₃₀ -b-PNIPAM ₂₂₇	31,277	43464	70,320	1.40	36.5

Table 2Molecular characteristics of PAA homopolymers.

Polymers	M _n (GPC) g/mol	M _w (GPC) g/mol	M _n (NMR) g/mol	PDI (GPC)
PAA ₃₅	4,076	4,507	2,522	1.11
PAA ₁₀₅	11,240	12,580	7,350	1.12
PAA ₂₆₁	24,459	28,568	18,807	1.17

 PAA_{102} , and PAA_{261} , respectively. The subscripts represented the DP for PAA. The molecular weights and polymer dispersity index (PDI) were determined by GPC, and results were showed in Table 2.

2.4. Membrane fabrication

Casting solutions were prepared by dissolving BCP into mixed solvents of different constitutions. The ratios of the carboxyl group (-COOH) to NIPAM unit ranged from 0 to 2, and the compositions of casting solutions were showed in Table 3. The well-dissolved solutions were left standing for more than 2 h to release air bubbles. The solution was then cast on a clean glass plate through a doctor blade with the gap height of $150\,\mu m$, then evaporated in the air for 15–90s, and finally transferred to de-ionized water. The temperature (25 °C) and humidity (40%) remained constant during membrane fabrication.

2.5. Flux and thermal-responsiveness determination

Fluxes were determined with a dead-end device under trans-membrane pressure of 0.1 MPa. The effective membrane area was $1.56\,\mathrm{cm}^2$. Electronic balance contained a water receiver was used to record the flux of permeate. The steady flux was obtained by compacting for 1 h. The water flux was calculated following Equation (1):

$$J = \frac{V}{A \cdot T} \tag{1}$$

where, the *J*, *V*, *A*, *T* corresponded to water flux, the volume of filtrate, the membrane area and the testing time, respectively.

Thermal responsiveness of the prepared membrane was determined by measuring the permeability under different temperatures. Before the test, the cell was allowed to stay at the set temperature for 1 h to ensure that the membrane had reached the test temperatures. Since the viscosity of water changed with temperature and affected the flux obviously, the flux calculated from Equation (1) was calibrated with viscosity. Here we used α to describe the degree of membranes thermal sensitivity, which was showed in Equation (2):

$$\alpha = \frac{J_t \cdot \mu_t}{J_{20} \cdot \mu_{20}} \tag{2}$$

where, α corresponded to the thermal sensitivity, J_t , J_{20} represented the water flux at t °C and 20 °C, respectively, and μ_t , μ_{20} were the viscosity of water at t °C and 20 °C, respectively.

2.6. General characterizations

Surface and cross-sectional morphologies were inspected by field emission scanning electron microscope (SEM, Hitachi 8010), and a thin layer of platinum (\sim 2 nm) was sputtered before observation. Microphase separation of BCPs in casting solution was analyzed by small angle X-ray scattering (SAXS, Xenocs), and details of this analysis were shown in our previous work [33]. Fourier transform infrared spectroscopy-attenuated total reflection (FTIR-ATR, iS50) was used to inspect the interaction of PAA with PS-b-PNIPAM in solutions. The measurement was conducted under a resolution of 4 cm $^{-1}$ from 32 scans.

3. Results and discussion

3.1. Membrane formation with additives

In a recent publication, PS-b-PNIPAM with the molecular weight of 194 kg/mol was fabricated into isoporous membranes using a mixture of DOX and THF, which was developed as the effective solvent that induces relatively well porous structure on membranes [23]. In the current work, the PS_{520-b-PNIPAM₁₃₉ with the molecular weight of 69.8 kg/mol was used to fabricate the membranes under identical conditions. Unfortunately, results in Fig. 1 indicate that the BCP used here cannot self-assemble into isoporous structures under the same}

Table 3Compositions of casting solutions for membrane preparation.

NO. BCPs	BCPs	Concentrations (wt%)	Additives	-COOH/NIPAM	Mixed Solvents (wt%)			
					DOX	THF	DMF	ACN
M1	PS ₅₂₀ -b-PNIPAM ₁₃₉	20	/	0	60	40	/	/
M2	PS ₅₂₀ -b-PNIPAM ₁₃₉	24	/	0	60	40	/	/
M3	PS ₅₂₀ -b-PNIPAM ₁₃₉	28	/	0	60	40	/	/
M4	PS ₅₂₀ -b-PNIPAM ₁₃₉	20	AA	1	60	40	/	/
M5	PS ₅₂₀ -b-PNIPAM ₁₃₉	20	CA	1	60	40	/	/
M6	PS ₅₂₀ -b-PNIPAM ₁₃₉	20	PAA ₁₀₂	1	60	40	/	/
M7	PS ₅₂₀ -b-PNIPAM ₁₃₉	20	PAA ₁₀₂	0.5	60	40	/	/
M8	PS ₅₂₀ -b-PNIPAM ₁₃₉	20	PAA ₁₀₂	2	60	40	/	/
M9	PS ₅₂₀ -b-PNIPAM ₁₃₉	20	PAA ₁₀₂	1	40	60	/	/
M10	PS ₅₂₀ -b-PNIPAM ₁₃₉	20	PAA ₁₀₂	1	80	20	/	/
M11	PS ₅₂₀ -b-PNIPAM ₁₃₉	12	PAA ₁₀₂	1	60	40	/	/
M12	PS ₅₂₀ -b-PNIPAM ₁₃₉	16	PAA ₁₀₂	1	60	40	/	/
M13	PS ₅₂₀ -b-PNIPAM ₁₃₉	24	PAA ₁₀₂	1	60	40	/	/
M14	PS ₅₂₀ -b-PNIPAM ₁₃₉	20	PAA ₃₅	1	60	40	/	/
M15	PS ₅₂₀ -b-PNIPAM ₁₃₉	20	PAA ₂₆₁	1	60	40	/	/
M16	PS ₄₃₀ -b-PNIPAM ₂₂₇	20	PAA ₃₅	1	60	40	/	/
M17	PS ₄₃₀ -b-PNIPAM ₂₂₇	20	PAA ₁₀₂	1	60	40	/	/
M18	PS ₄₃₀ -b-PNIPAM ₂₂₇	20	PAA ₂₆₁	1	60	40	/	/
M19	PS ₅₁₅ -b-PNIPAM ₃₂	20	PAA ₃₅	1	60	40	/	/
M20	PS ₅₁₅ -b-PNIPAM ₃₂	20	PAA ₁₀₂	1	60	40	/	/
M21	PS ₅₁₅ -b-PNIPAM ₃₂	20	PAA ₂₆₁	1	60	40	/	/
M22	PS ₅₂₀ -b-PNIPAM ₁₃₉	20	PAA ₁₀₂	1	90	/	10	/
M23	PS ₅₂₀ -b-PNIPAM ₁₃₉	20	PAA ₁₀₂	1	90	/	/	10
M24	PS ₅₂₀ -b-PNIPAM ₁₃₉	22	PAA ₁₀₂	1	90	,	,	10

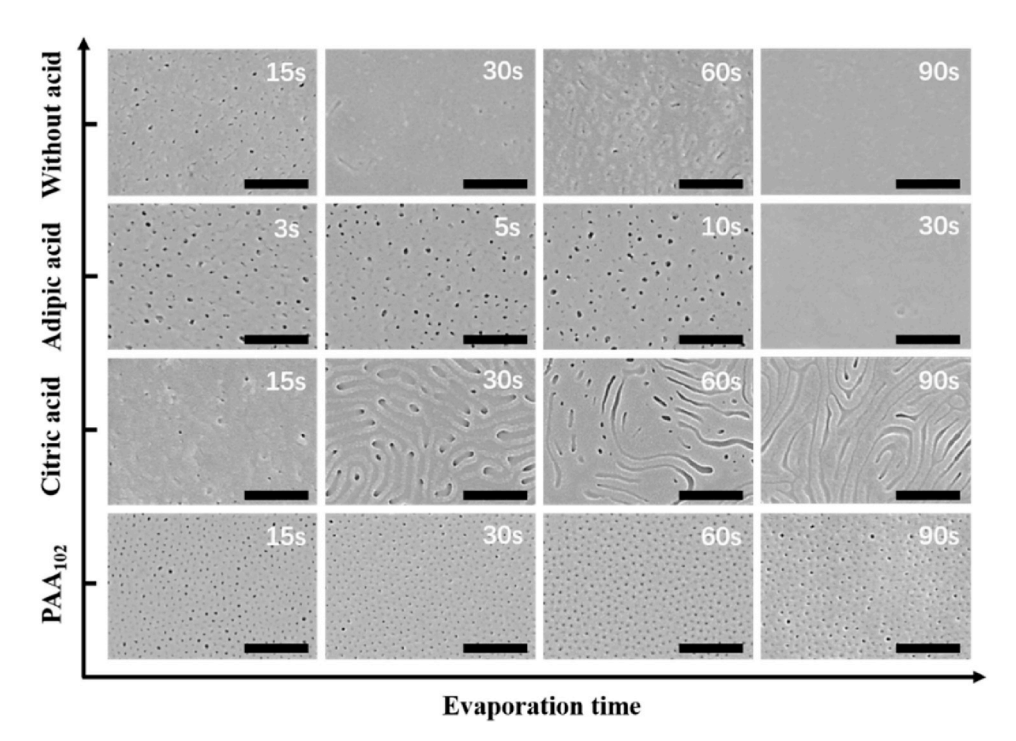


Fig. 1. SEM images of membranes prepared from blending with different acids. The molar ratio of -COOH/NIPAM is 1:1. The scale bar in the image is 300 nm.

condition with literature. The reason can be assigned to its lower molecular weight that has decreased the segregation strength of blocks in solutions

It is previously found that small molecules such as polyols and organic acids will promote the self-assembly of BCP in solution [29,34,35]. Therefore, small molecules containing -COOH are firstly tested as additives for PS-b-PNIPAM (Scheme 1), and their effects on membrane formation are investigated. The molecules containing -COOH are selected because the amide group in NIPAM is a well-known hydrogen bond acceptor (H-acceptor) that tends to form molecular interactions with H-donor species. The additive is added at the molar ratio of -COOH/NIPAM (1:1), and concentrations as well as the solvent for membrane fabrication remain unchanged. Results in Fig. 1 indicate that the adipic acid is just a pore-forming agent for the BCP, which makes the membranes become porous while polymer assembly is not observed. The surface becomes dense and poreless with the increase of evaporation time. The citric acid (a ternary acid) does promote the selfassembly, and worm-like structure is generated with the prolongation of evaporation time, indicating that the density (or number) of -COOH in molecules may be a factor that affects the self-assembly. Therefore, we move to polymers or macromolecules containing -COOH groups. Surprisingly, when poly (acrylic acid) with the DP of 102 is added as the additive, the isoporous structure is clearly induced. The pore density of prepared membranes reaches $7.54 \times 10^{14}/\text{m}^2$ (30s) and 5.37×10^{14} /m² (60s), which is on the same order with that found for membranes prepared from high γ BCPs such as PS-b-P4VP. It is worth noting that the pores on membranes fabricated under the optimized condition have shown an excellent pore uniformity, and pores on PS-b-PNIAPM membranes prepared herein display the uniformity similar to PS-b-P4VP membranes when their size are the same [30].

To prove that the formation of isoporous structure is truly related to

Scheme 1. Molecular structure of different additives.

PAA, the effect of PAA contents on membrane formation has been further studied. The molar ratio of -COOH to NIPAM is changing from 0:1, 0.5:1, 1:1 to 2:1, which corresponds to a mass ratio of 0%, 7%, 14%, and 28% for the PAA₁₀₂/PS₅₂₀-b-PNIPAM₁₃₉. The structure of membranes formed under these ratios is shown in Fig. 2, which indicates that the isoporous structures are successfully induced at all the set contents. By comparing the structure generated at the evaporation time of 15 and 30 s, it can be found that the contents of the additive show a remarkable impact on membrane formation. At the -COOH/ NIPAM of 0.5:1, rather dense surface is found although the BCP shows a tendency to assemble into isoporous structures, and relatively ordered pores are generated when the evaporation time increase to 60 and 90 s. Since the viscosity increases sharply at the -COOH/NIPAM of 2:1, the casting solution is diluted to 16 wt%. It is amazing to found that the membrane generated from this diluted concentration still show good isoporous structures, implying that PAA added to solution has played an important role in membrane formation. A careful analysis of SEM images in Fig. 2 indicates that the pore sizes show a close dependent on amounts of PAA feed to the solution. At the evaporation time of 60s, the pore size for the membranes generated at the -COOH/NIPAM ratio of 0.5:1, 1:1 and 2:1 are 9.84, 10.64, and 11.81 nm, respectively.

3.2. PAA induced phase separation

For the well-defined SNIPS process, generation of isoporous membranes usually resulted from the microphase separation of BCPs dissolved in solutions. In the current work, the casting solutions with and without additives are analyzed by SAXS, which is known for its sensitivity to the microphase separation of polymers in bulk or solutions. For the control solution without PAA (Fig. 3), the SAXS curve decays smoothly with an increase of scattering vector (q), and no peak can be found along with the profile. This result indicates that PS₅₂₀-b-PNIPAM₁₃₉ has not undergone microphase separation in casting solution, which explains the reason why isoporous membranes cannot generate from this solution (20 wt%). However, when PAA is added at a molar ratio of –COOH/NIPAM = 1/1, clear scattering peaks are found, implying that the microphase separation of BCP has been successfully induced. It is worth noting that two peaks observed on the SAXS profile

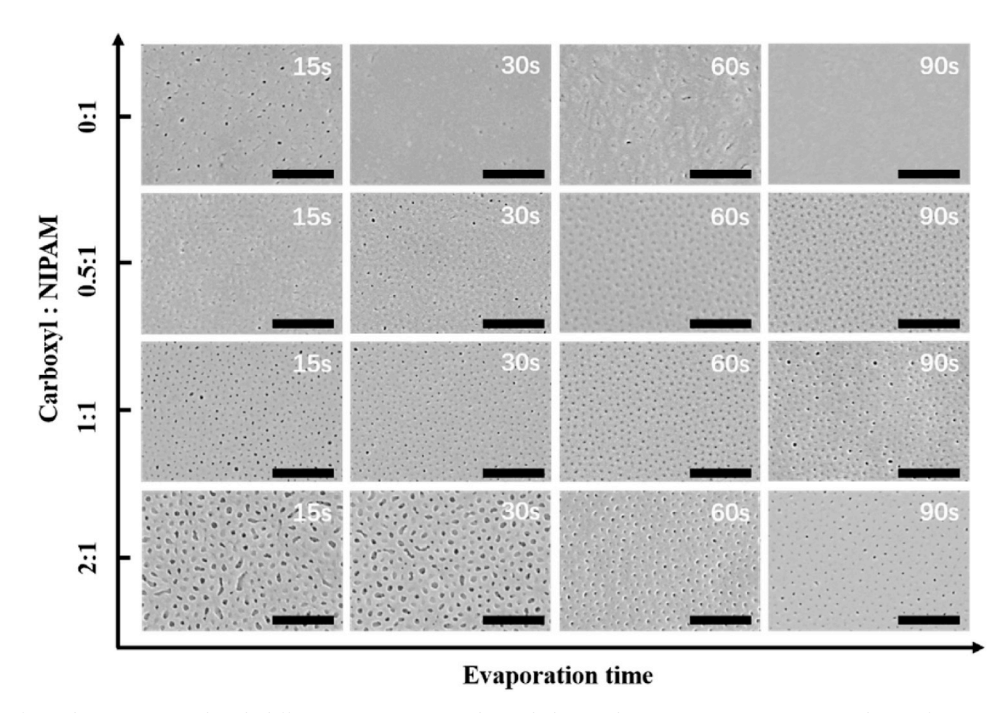


Fig. 2. SEM images of membranes prepared with different PAA contents. The scale bar in the image is 300 nm. PAA with DP of 102 was used as the additive.

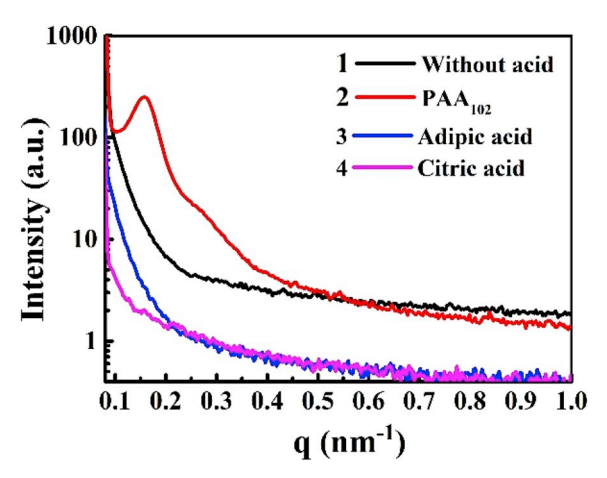


Fig. 3. SAXS profiles for the casting solutions with and without additives. The molar ratio of -COOH/NIPAM is 1/1. A mixture of 60 wt% DOX and 40 wt% THF was used as the solvent.

display a ratio of 1: $\sqrt{3}$ that corresponds closely to packed hexagonal nano-structure [9], which agrees well with the pore arrangement found on membranes. Besides, the *d-spacing* of micro-domains determined in solutions (40 nm) in line with the *d-spacing* of neighbor pores on membranes (35.1 \pm 2 nm, with the evaporation time of 60s), implying again that the formation of isoporous membranes is closely related to the microphase separation of BCP in solutions. However, for the controlled samples with adipic acid and citric acid as additives, no scattering can be found, indicating the small organic acids are unable to induce the microphase separation of PS-b-PNIPAM in solutions. This result differs significantly from the finding observed for PS-b-P4VP, the microphase separation of which in solutions can be easily induced by small organic acids [30].

It's interesting to explain the finding why the microphase separation of PS-b-PNIPAM can be induced by PAA. We firstly interpreted it from the solubility parameter. As is showed in Table 4, it can be easily found that the PS and PNIPAM share a very close solubility parameter (δ_{total}), implying that the Flory-Huggins interaction parameter of them tends to be small. This expression explains the undetectable microphase

Table 4Solubility parameters of polymers, solvent, and additives used in this work.

	$\delta_{total}~(\text{MPa}^{0.5})$	δ_d (MPa ^{0.5})	$\delta_p \; (MPa^{0.5})$	$\delta_h \; (MPa^{0.5})$
PS [13]	18.60	_	_	_
PNIPAM [36]	19.64	-	_	8.9 ^a
PAA [37]	28.20	17.3	12.2	18.6
DOX [38]	20.47	19.0	1.8	7.4
THF [38]	19.46	16.8	5.7	8.0
DMF [38]	26.63	17.4	16.7	11.3
ACN [38]	24.40	15.3	18	6.1
χ (PS-PNIPAM)	0.047			

^a For NIPAM monomer [39].

separation for PS-b-PNIPAM in solution (Fig. 3). However, the solubility parameter of PAA differs largely from that of PS, indicating that PAA will not show a preferential interaction with PS. More importantly, the notably big H-bonding components of PAA and PNIPAM indicate that they are both good H-bonding formers and tend to interact with each other. However, the interaction of PAA with PNIPAM in organic solvent hasn't been intensively determined, although their H-bonding have been proved in aqueous solutions before [32].

To directly inspect the possible interaction of PAA with PNIPAM, casting solutions used for membrane fabrication are analyzed by FT-IR. Herein we focus on the vibrations from [C=O-(N-H)] group in PNIPAM and the [(C=O)-O-H] group in PAA. Fig. 4 indicates that the C=O-(N-H) and (C=O)-O-H show the characteristic wavenumbers around 3311 cm⁻¹ and 1736 cm⁻¹, respectively for the control solutions with only BCP and PAA. However, the vibration for C=O-(N-H) (3311 cm⁻¹) has shifted to higher wavenumbers (3324 cm⁻¹) when PAA is introduced. Meanwhile, the vibration of (C=O)-O-H that originally appears at 1736 cm⁻¹ shifts to 1726 and 1708 cm⁻¹ for the PAA in the casting solution. Obviously, the shift of vibrations from both NIPAM and PAA demonstrates that they interact with each other in the casting solution [32,40].

FT-IR analysis provides clear evidence on the H-bonding interaction of PAA with PNIPAM. Theoretically, the selective interaction of PAA with PNIPAM will contribute to the microphase separation of BCP in different ways. Firstly, the Flory-Huggins parameter ($\chi = 0.18$) of PAA and PS is obviously larger than that of PNIPAM and PS ($\chi \approx 0.05$, S

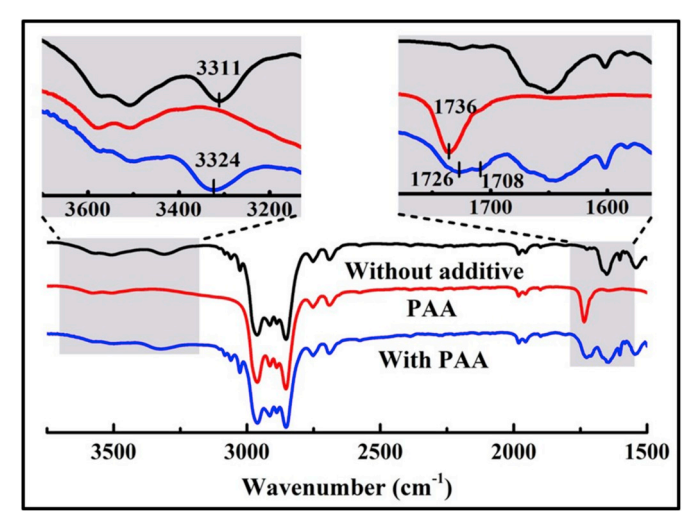
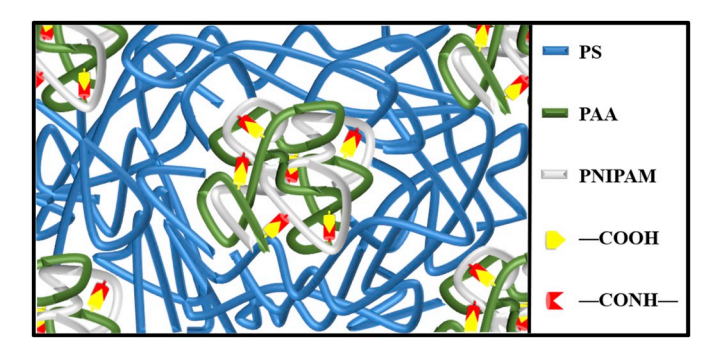


Fig. 4. FTIR spectra of casting solution containing PAA. Solutions with only PAA and PS-b-PNIPAM served as control samples.

2.2). Loading of PAA to PNIPAM will obviously increase the phase repulsion between the PS and complex of (PNIPAM + PAA). Secondly, the multivalent H-bonding interaction, which arises from PAA and PNIPAM, will stabilize the phase separation more effectively than small organic acids if phase separation is successfully induced. The stabilization of small molecules on phase separated domains has been found for PS-b-P4VP before [30]. This stabilization effect for PS-b-PNIPAM is also expected for the organic acids used in the current work. However, one of the reasons why small organic acids cannot induce the phase separation may result from their weak stabilization ability for the PS-b-PNIPAM. This analysis explains why isoporous structure can be only generated from PAA rather than the small organic acids.

Scheme 2 is provided to help understand the explanation for the PAA induced microphase separation. From Scheme 2, we can interpret that the multivalent H-bonding interaction between PAA and PNIPAM make them bind tightly to each other, which will obviously stabilize the microphase if self-assembly is induced. In addition, the loading of the PAA to PNIPAM phase will increase the fractions of the hydrophilic phase. As a result, the pore size that derives from the hydrophilic phase will be increased with an increase in feeding amounts of PAA. This explains the pore size evolution found by SEM image showed in Fig. 2. Charles previously observed in thin films that domain size could be facilely adjusted with changing the amount of additive loaded to PEO phase [41]. However, their work concentrated on dried films which did not suffer from the competition from solvents. Our result indicates that the selective interaction of PAA with PNIPAM in solutions will simultaneously induce the phase separation and increase the pore (domain) size of weakly separated copolymers, which are critically important for the fabrication of membranes from those BCPs belonging to



Scheme 2. A possible mechanism for the PAA induced microphase separation of PS-*b*-PNIPAM.

low χ polymers.

3.3. MW effect of PAA on isoporous formation

To extend the observation that was found for PS₅₂₀-b-PNIPAM₁₃₉, we further study the membrane formation from another two BCPs of different molecular weights and compositions. Another two PAA with different polymerization degrees, PAA35 and PAA261, were used as additives for BCPs. The surface morphologies are shown in Fig. 5 (more results for membranes prepared at an evaporation time of 30s are presented in Fig. S3). Fig. 5 clearly indicates that the newly synthesized BCPs, PS₄₃₀-b-PNIPAM₂₂₇, and PS₅₆₀-b-PNIPAM₃₂, cannot self-assemble into isoporous membrane without additive. This result is consistent with what has been observed for PS₅₂₀-b-PNIPAM₁₃₉. In contrast, they readily assemble into isoporous structures when PAA of proper molecular weights are added as additives, demonstrating that the co-assembly strategy proposed in this work is effective. Although PS-b-PNIPAM copolymers can be all fabricated into isoporous membranes with the aid of PAA, their dependence on the MWs of PAA are obviously different. For the PS₅₂₀-b-PNIPAM₁₃₉, much better isoporous structures have been found for PAA with the DPs of 102 and 261, although isoporous structure can be generated from all three PAA with the DPs ranging from 35 to 261. A similar result is found for PS₅₆₀-b-PNIPAM₃₂, which self-assembles into relatively better isoporous structures with the PAA having DPs of 35 and 102. For the third BCP, PS₄₃₀-b-PNIPAM₂₂₇, it assembles into the best isoporous structures only when the DP of PAA is close to that of PNIPAM. From these morphologies showed in Fig. 5, it seems that the best isoporous structures tend to be generated at the DPs of PAA closing to that of PNIPAM in BCPs.

To understand the effect of PAA on polymer assembly, casting solutions containing PAA of different DPs are investigated by SAXS. Fig. 6 shows that the microphase separation of PS-b-PNIPAM is strongly dependent on the MWs of PAA added to the solution. For the PS₅₂₀-b-PNIPAM₁₃₉, the microphase separation is obviously induced by both the PAA₃₅ and PAA₁₀₂. However, when SAXS profiles are carefully compared, we will find that PAA₁₀₂ leads to obviously larger d-spacing because of the smaller q. Besides, a secondary peak is found for the solution containing PAA₁₀₂, which indicates that a better domain ordering has been induced in solutions. It is easy to understand this result from the aspect of segregation strength (χN) that is usually considered as the driving force for microphase separation. For the PAA interacting with PNIPAM and loaded to the corresponding phase, the phase repulsion from PS will increase with an increase of the DP. Therefore, better-organized domains are induced for the solution containing PAA₁₀₂. Unfortunately, the PAA with DP of 261 cannot dissolve well in the selected solvent, and casting solution with PAA261 become turbid (Fig. S4). This might be a reason for the undetectable scattering for the solutions containing PAA261. However, although the PAA with DP of 261 dissolves poorly in the selected solvent, its contribution on isoporous formation is still found for PS520-b-PNIPAM139 and PS430-b-PNIPAM₂₂₇, possibly indicating that the few PAA dissolved into solution also increases polymer assembly during membrane formation.

Besides the contribution on inducement of the microphase separation, the stabilization on phase separated domains from PAA is another factor that might affect the final structure. The stabilization is related to the interaction between PAA and PNIPAM that will restrict the chain mobility during membrane formation. Typically, the larger MW of PAA, the stronger restriction to PNIPAM will become. For PS $_{520}$ -b-PNIPAM $_{139}$, the membranes prepared with additives of PAA $_{35}$, PAA $_{102}$ and PAA $_{261}$ show obviously decreasing pore size. For the PS $_{520}$ -b-PNIPAM $_{32}$, a similar result is found if the pore size of membranes prepared with the PAA $_{261}$ is taken as zero (No pores are found on this membrane). Dami found in their publication that radius of isopores in the resulting membrane prepared from SNIPS is similar to the hydrodynamic diameter of the pore-forming block [42]. Considering that PAA with larger MWs has shown a decreased solubility in casting

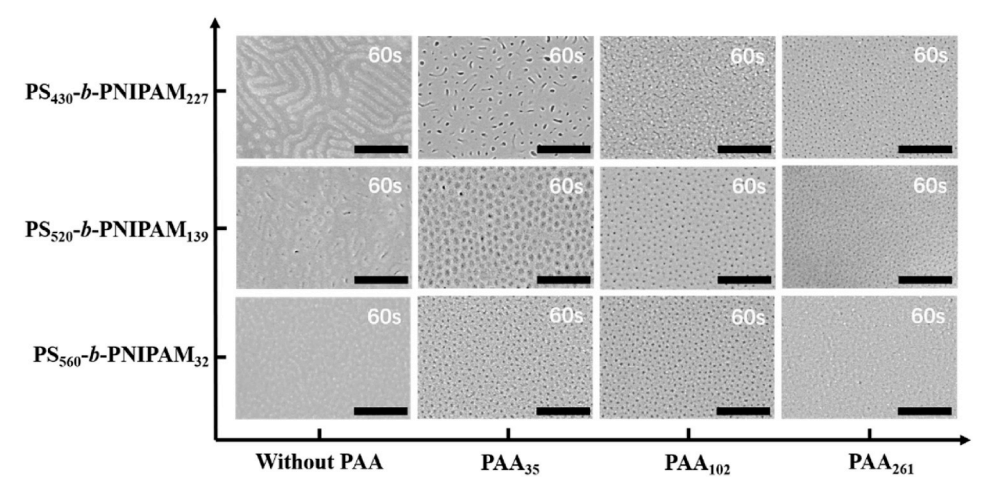


Fig. 5. SEM images of membranes prepared from different BCPs with different additives. The molar ratio of -COOH/NIPAM is 1:1. Scale bars in images are 300 nm.

solution, PAA loaded to PNIPAM domains will make the PNIPAM phase become more compact for those PAA with higher MWs. Eventually, it will lead to decreased pore size.

The condition for PS₄₃₀-b-PNIPAM₂₂₇ is a little different but can be similarly explained. The PS430-b-PNIPAM227 itself assembles into parallel cylindrical structures without additives. However, with the introduction of PAA, the parallel cylindrical structures gradually turn into vertical isoporous when MWs of PAA increase. The SAXS results of casting solutions prepared from blending with PAA_{35} and PAA_{102} show similar scattering. However, the final structures on membranes are different. The results can be related to the stronger stabilization effect of larger PAA that has retained the assembled structure during the membrane formation. In fact, the structural evolution, especially the transition from assembly to disassembly, is rather common for the welldefined SNIPS. However, this transition can be effectively prevented by the additives that show stabilization to polymer phase [30]. For the PS₄₃₀-b-PNIPAM₂₂₇, the PAA with DP of 102 seems to play dual roles of inducement of phase separation and the stabilization of phase separated domains. The stabilization of PAA261 to PNIPAM phase is also expected although it dissolves only partly in the casting solution.

3.4. Membrane formation at different concentrations

It has been reported that isoporous membranes can be generated at or slightly below the critical micelle concentration of BCPs dissolved in solution [43]. From a practical point of view, it is desirable to figure out the lowest concentration that leads to the isoporous structure as this condition will both increase membranes permeability and decrease the consumption of BCPs. The membranes are therefore prepared from

concentrations ranging from 8 to 24 wt% to find out the evolution of membranes structure with concentrations. Results in Fig. 7 clearly indicates that isoporous structures are well induced even though the concentration is lowered down to 12 wt%, stressing the function of PAA induced self-assembly. As displayed in Fig. 1, the PS₅₂₀-b-PNIPAM₁₃₉ itself cannot self-assemble into isoporous membranes at the concentration of 20 wt%, indicating that the critical micellization concentration of PS₅₂₀-b-PNIPAM₁₃₉ should be higher than 20 wt% (Fig. 6). As thus, it can be excepted that the polymer itself is unable to selfassemble into isoporous structures at 12 wt% without PAA, neither. At the same time, we find that isoporous membrane is also generated at the concentration of 24 wt% via the blending method. However, membrane prepared from pure BCP at this concentration does not show isoporous structures (Fig. S5), indicating the formation of isoporous membranes under this concentration still results from the functions of PAA. Therefore, results in Fig. 9 clearly demonstrate that the self-assembled, isoporous membranes can be generated from a broad concentration range with the aid of PAA additive. This finding is beneficial to the adjustment of membranes mechanical strength as well as the microstructure (pore size, porosity, and et al.) by just changing the solution concentrations.

Besides the effect of fabrication concentration, we observed that the membranes permeability and pore size are notably affected by the MWs of PAA applied (Table 5). For the membrane M14, M6 and M15 that are prepared at the same concentration but with different PAA polymers, their permeability and pore size decrease obviously with an increase of MW of PAA. It is also interesting to compare our results with the recent publication. Merve fabricated isoporous membranes using the PS-b-PNIPAM with MW of 194 kg/mol as material. They found that relatively

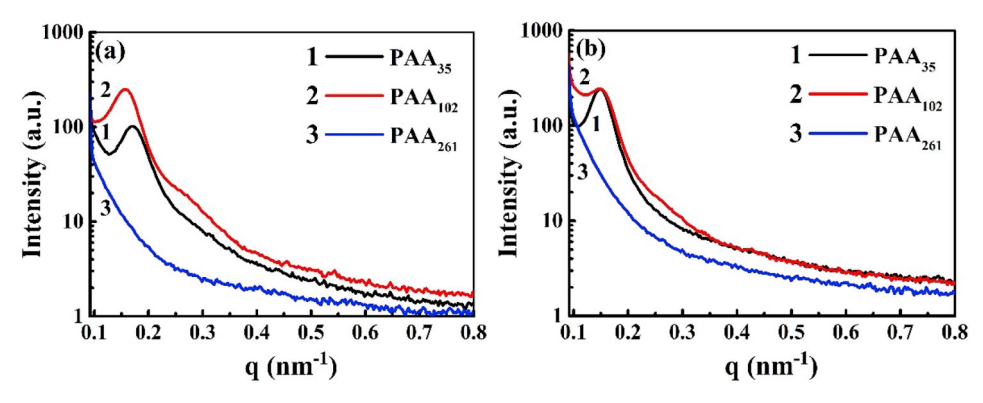


Fig. 6. SAXS profiles of the casting solutions prepared from (a) PS_{520} -b-PNIPAM₁₃₉ and (b) PS_{430} -b-PNIPAM₂₂₇. PAA with different DPs are used as additives. The molar ratio of -COOH/NIPAM remains constant at 1:1 for all the solutions.

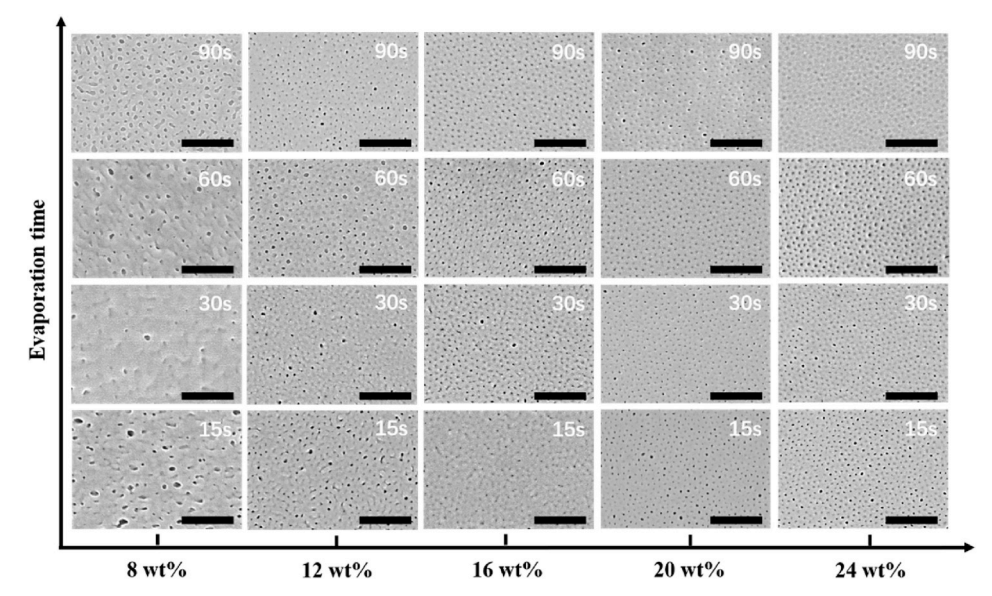


Fig. 7. SEM images of membranes prepared from different concentrations. PAA₁₀₂ was used as an additive. The molar ratio of -COOH/NIPAM is 1:1. The scale bar in the image is 300 nm.

well organized isoporous structures was generated at concentrations higher than 20 wt%, and their membranes presented notably larger pore size of 18.5 nm because of the higher MW, and permeability of their membranes was only $\sim 2\,\mathrm{L\,m^{-2}.bar^{-1}.h^{-1}}$. However, our membrane displays an obviously larger permeability although the pore size is much smaller (9.35 nm). The loose and porous structures in cross-section caused by PAA additive may be a reason for this improvement (Fig. S6). This comparison also demonstrates the fundamentally important role of PAA on the inducement of surface and internal porosity. Table 5 implies clearly that the co-assembly with PAA has provided a facile while effective way to adjust the pore size and permeability of membranes prepared from PS-b-PNIPAM.

The separation performance of prepared membranes (M6-30s) is carried out. The rejections to lysozyme (4.5 nm) and hemoglobin (6.4 nm) in their mixture are determined to be 41% and 95%, respectively, demonstrating the sub-10 nm pores of fabricated membranes as well as its potential in precise molecular separation. The spectra for protein solutions before and after the separation are showed in Fig. S7.

3.5. Membrane formation from newly developed solvents

Until now, PS-b-PNIPAM can be only fabricated into isoporous membrane with the mixed solvent consisting of DOX and THF. With the demonstrated co-assembly strategy in hand, it is possible to extend the solvent species that can be used in membrane fabrication. Thus, we try the new combinations of DOX with DMF or acetonitrile (ACN). DMF is considered because it displays a much higher polarity, which will increase the solvent/non-solvent (H₂O) exchange during phase inversion and eventually increase membranes porosity. Unfortunately, it was found that polymer assembly is largely destroyed even though only 10 wt% DMF is introduced to DOX (Fig. S8). The reason may be related to its competitive H-bonding ability that will weaken the interaction of PAA with PS-b-PNIPAM (Table 4). Therefore, we move to ACN that has a similar Hansen solubility parameter with DMF but its H-bonding component is much smaller. Surprisingly, well organized isoporous structures are readily generated from mixed solvent consisting of 90 wt % DOX and 10 wt% CAN (Fig. 8, Fig. S9 shows the membranes prepared at 20 wt%.). More importantly, the membrane prepared from this

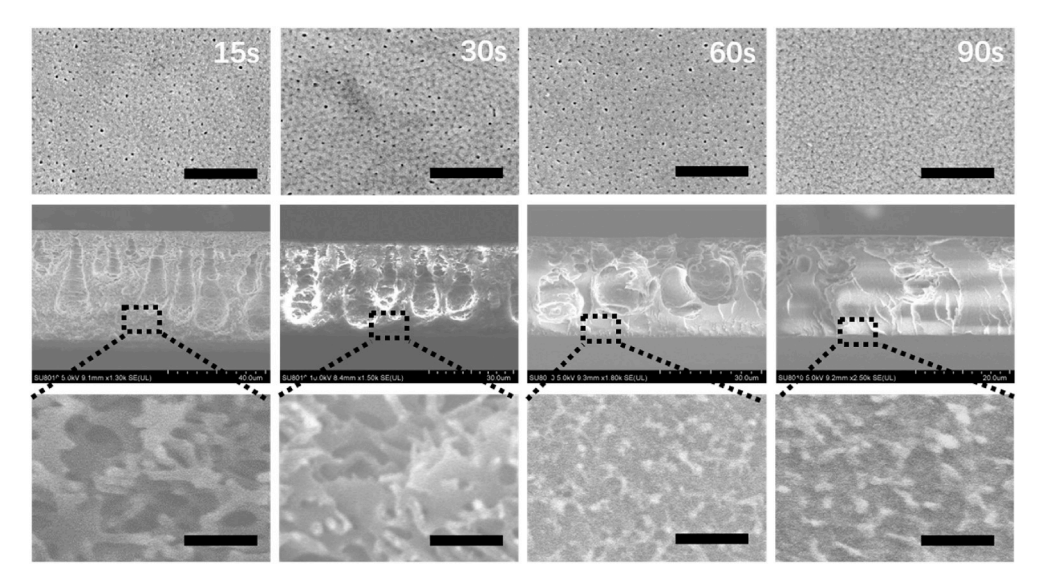
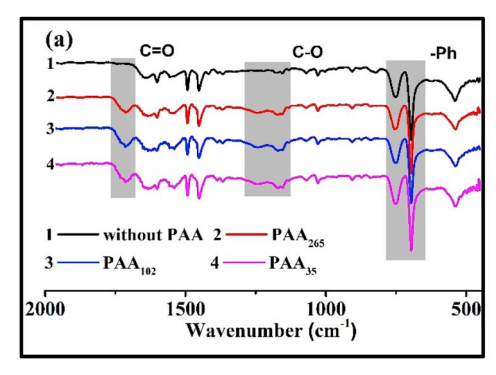


Fig. 8. SEM images of membranes prepared from a mixture of DOX and ACN. PAA₁₀₂ was used as the additive, and the molar ratio of -COOH to NIPAM is 1:1. Solution concentration is 22 wt%. The scale bar in the image is 300 nm.



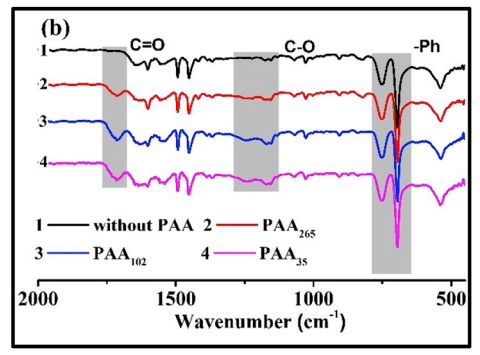


Fig. 9. FT-IR results for membranes prepared with PAA of different MWs. The molar ratio of -COOH/NIPAM is 1:1. Evaporation time in (a) and (b) is 30 and 60 s, respectively.

solvent shows a typical asymmetric structure that is usually found for the SNIPS (Fig. 8). The permeability of membranes generated at the evaporation time of 30s reached 20.11 L/h·m²-bar, which is 1.76 and 10.06 times larger than the M6 and the membrane showed in literature [23], indicating that the permeability and porosity in the cross-section can be further improved by using solvents differing from the DOX/THF combination. The sublayer close to the bottom surface becomes denser when evaporation time increases to 60s although the isoporous structure is still found on the surface. As thus, the permeability of membranes prepared from 60s is not determined.

3.6. Membrane composition and performance

The compositions of isoporous membranes prepared from blending with PAA are analyzed by FT-IR. Fig. 9 indicates that the signal from carboxyl groups is clearly detectable, implying that there are some PAAs reserved in the membranes. Taking the signal of the benzene group from PS block as the internal standard, the amount of PAA reserved in membranes can be estimated by integrating the signal intensity of the carboxyl group to the benzene group. Herein, the result from fully dried membrane without phase inversion is taken as reference. From the results shown in Table 6, it can be found that the longer the evaporation time is, the higher the retention rate becomes. This is because the solution gets concentrated with the increase of solvent evaporation time, which makes it much more difficult for PAA to migrate from membranes during the phase inversion. Besides, it is also found that the residual amounts of PAA follow the order of M6 > M14 > M15. For the M6 and M14, the amounts of PAA reservation are mainly dependent on their molecular weights. As the MW of PAA₁₀₂ is much higher, it will deliver stronger interaction with BCPs, which will lead to higher retention. For the PAA261, however, its solubility in casting solution is relatively poor. The H-bonding interaction of PAA₂₆₁ with PS-b-PNIPAM is discounted. As a result, it can be much easier to be washed out from membranes during phase inversion. This result is to some extent consistent with the results found by SAXS.

Finally, the thermal-responsive behavior of prepared membranes is studied. To describe the membranes thermal-responsiveness in a much more precise way, the flux presented here is calibrated with the water viscosity (Equation (2)). Fig. 10 (a) clearly indicates that flux increases

Table 6Contents of PAA reserved in isoporous membranes.

Evaporation Time	M ₁ (without PAA)	M ₁₄ (PAA ₃₅)	M ₆ (PAA ₁₀₂)	M ₁₅ (PAA ₂₆₁)
30 s	0.0	69.0%	83.9%	45.0%
60 s	0.0	76.0%	87.3%	68.3%

sharply at the temperature between 25-35 °C, which is consistent with the low critical solution temperature (LCST, \sim 32 °C) of PNIPAM [44–46]. The increase of flux is thus mainly ascribed to the broadening of pore size that is related to the shrinkage of PNIPAM chains. Fig. 10 indicates that the thermal-responsiveness remains unaffected although there are some PAAs reserved in membranes. The repeated determination from several cycles shifted repeatedly from 20 to 40 °C also proves that prepared membranes give stable thermal responsiveness. This behavior can be used to fabricate fouling-resistance and self-cleaning isoporous membranes.

4. Conclusions

To summarize, PS-b-PNIPAM that belonged to low γ BCPs was successfully fabricated into isoporous membranes through the co-assembly with PAA. Typically, with the co-assembly strategy, isoporous membranes were able to generate from PS-b-PNIPAMs of relatively low molecular weights (70 kg/mol) at less concentrated solutions (≤20 wt %). The result was assigned to the PAAs that had contributed to the microphase separation of BCPs by selectively interacting with PNIPAM. Isoporous membranes were successfully prepared from all three BCPs having different molecular weights and compositions, demonstrating the effectiveness and universality of the co-assembly strategy. With the aid of PAA, the membrane was able to fabricate from different solvents and a wide range of concentrations, opening the way for tailoring the pore size and permeability of isoporous membranes. In comparison with the membrane prepared from similar BCPs, our membranes presented obviously higher permeability although isopores on the surface were much smaller, indicating the functions of PAA on tailoring both the surface and internal structures. Finally, the thermal-responsiveness of prepared isoporous membranes were studied and found that the PAA

Table 5Water flux and pore size of isoporous membranes prepared with the PAA additives.

Membrane ^a	M1 (without PAA)	M14 (PAA ₃₅)	M6 (PAA ₁₀₂)	M15 (PAA ₂₆₁)	M24 (PAA ₁₀₂)
Pore size (nm) ^b	13.81	13.13	9.35	8.69	9.02
Porosity (%) ^b	0.60	11.18	5.40	5.42	4.01
Permeability (L·m ⁻² ·h ⁻¹ ·bar ⁻¹)	0.84	13.38	11.40	8.24	20.11

^a With the evaporation time of 30s.

^b Analyzed by Image J (version 5.0).

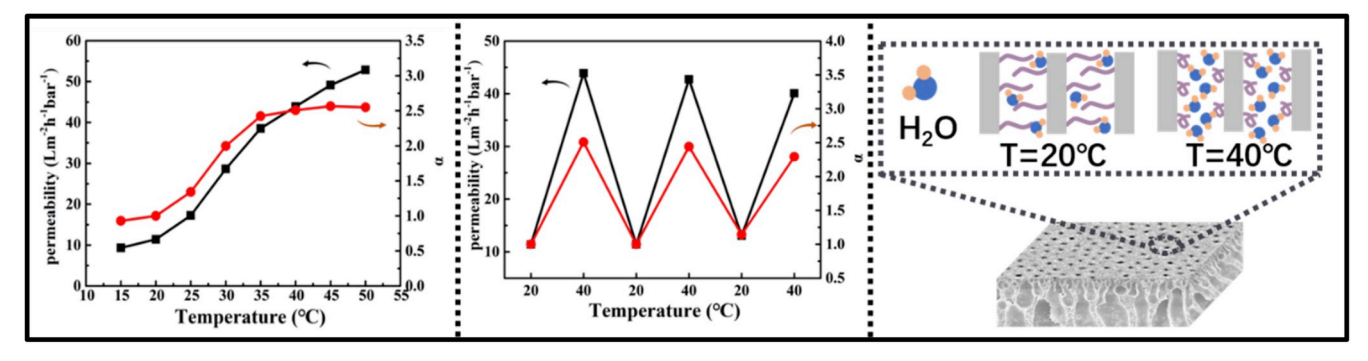


Fig. 10. Thermal-sensitive behavior of the prepared membrane.

reserved in membranes did not affect the membranes thermal-responsive behavior. The strategy showed in current work had provided a facile and reliable method to prepare isoporous membranes from BCPs belonged to low χ polymers.

Acknowledgments

Financial supports from the Natural Science Foundation of Zhejiang Province (LQ16B040002), National Natural Science Foundation of China (21506186). The Public Welfare Project of the Science and Technology Committee of Zhejiang Province (LGG19B060001) and the Founding from China Scholarship Council (CSC) were sincerely acknowledged.

Appendix A. Supplementary data

Supplementary data to this article can be found online at https://doi.org/10.1016/j.memsci.2019.117255.

References

- G. Belfort, Membrane filtration with liquids: a global approach with prior successes, new developments and unresolved challenges, Angew. Chem. 131 (2019) 1892–1902
- [2] R.C. Furneaux, W.R. Rigby, A.P. Davidson, The formation of controlled-porosity membranes from anodically oxidized aluminium, Nature 337 (1989) 147–149.
- [3] H. Xu, W.A. Goedel, From particle-assisted wetting to thin free-standing porous membranes, Angew. Chem. 42 (2003) 4694–4696.
- [4] W. Starosta, D. Wawszczak, B. Sartowska, M. Buczkowski, Investigations of heavy ion tracks in polyethylene naphthalate films, Radiat. Meas. 31 (1999) 149–152.
- [5] M.E. Warkiani, C. Lou, H. Liu, H. Gong, A high-flux isopore micro-fabricated membrane for effective concentration and recovering of waterborne pathogens, Biomed. Microdevices 14 (2012) 669–677.
- [6] P. Weiss, Block copolymers overview and critical survey, Allen Noshay and James E. Mcgrath, Academic, New York, 1977, 516 pp, J. Polym. Sci., Polym. Lett. Ed. 16 (1978) 151–152.
- [7] K. Peinemann, V. Abetz, P.F.W. Simon, Asymmetric superstructure formed in a block copolymer via phase separation, Nat. Mater. 6 (2007) 992–996.
- [8] E.A. Jackson, M.A. Hillmyer, Nanoporous membranes derived from block copolymers: from drug delivery to water filtration, ACS Nano 4 (2010) 3548–3553.
- [9] R.M. Dorin, D.S. Marques, H. Sai, U. Vainio, W.A. Phillip, K. Peinemann, S.P. Nunes, U. Wiesner, Solution small-angle X-ray scattering as a screening and predictive tool in the fabrication of asymmetric block copolymer membranes, ACS Macro Lett. 1 (2012) 614–617.
- [10] W.A. Phillip, M.A. Hillmyer, E.L. Cussler, Cylinder orientation mechanism in block copolymer thin films upon solvent evaporation, Macromolecules 43 (2010) 7763–7770
- [11] S.P. Nunes, A.R. Behzad, K. Peinemann, Self-assembled block copolymer membranes: from basic research to large-scale manufacturing, J. Mater. Res. 28 (2013) 2661–2665.
- [12] M. Radjabian, V. Abetz, Tailored pore sizes in integral asymmetric membranes formed by blends of block copolymers, Adv. Mater. 27 (2015) 352–355.
- [13] S. Rangou, K. Buhr, V. Filiz, J.I. Clodt, B. Lademann, J. Hahn, A. Jung, V. Abetz, Self-organized isoporous membranes with tailored pore sizes, J. Membr. Sci. 451 (2014) 266–275.
- [14] G.O.R.A. Van Ekenstein, R. Meyboom, G.T. Brinke, O. Ikkala, Determination of the Flory-Huggins interaction parameter of styrene and 4-vinylpyridine using copolymer blends of poly(styrene-co-4-vinylpyridine) and polystyrene, Macromolecules 33 (2000) 3752–3756.
- [15] W. Zha, C.D. Han, D.H. Lee, S.H. Han, J.K. Kim, J.H. Kang, C. Park, Origin of the

- difference in Order Disorder transition temperature between polystyrene-block-poly(2-vinylpyridine) and polystyrene-block-poly(4-vinylpyridine) copolymers, Macromolecules 40 (2007) 2109–2119.
- [16] J. Cheng, R.A. Lawson, W.-M. Yeh, N.D. Jarnagin, L.M. Tolbert, C.L. Henderson, PS-b-PHEMA: Synthesis, Characterization, and Processing of a High X Polymer for Directed Self-Assembly Lithography, SPIE, 2013.
- [17] J. Cheng, R.A. Lawson, W. Yeh, N.D. Jarnagin, A.J. Peters, L.M. Tolbert, C.L. Henderson, Directed self-assembly of poly(styrene)-block-poly(acrylic acid) copolymers for sub-20nm pitch patterning, Proc. SPIE (2012) 8323.
- [18] T.P. Russell, P.R. Hjelm, P.A. Seeger, Temperature dependence of the interaction parameter of polystyrene and poly(methyl methacrylate), Macromolecules 23 (1990) 890–893.
- [19] A.S. Zalusky, R. Olayovalles, J.H. Wolf, M.A. Hillmyer, Ordered nanoporous polymers from Polystyrene Polylactide block copolymers, J. Am. Chem. Soc. 124 (2002) 12761–12773.
- [20] T.H. Epps, T.S. Bailey, R. Waletzko, F.S. Bates, Phase behavior and block sequence effects in lithium perchlorate-doped poly(isoprene-b-styrene-b-ethylene oxide) and poly(styrene-b-isoprene-b-ethylene oxide) triblock copolymers, Macromolecules 36 (2003) 2873–2981
- [21] W. Young, T.H. Epps, Salt doping in PEO-containing block copolymers: counterion and concentration effects, Macromolecules 42 (2009) 2672–2678.
- [22] M. Karunakaran, S.P. Nunes, X. Qiu, H. Yu, K. Peinemann, Isoporous PS-b-PEO ultrafiltration membranes via self-assembly and water-induced phase separation, J. Membr. Sci. 453 (2014) 471–477.
- [23] M. Mocan, H. Wahdat, H.M.V. Der Kooij, W.M. De Vos, M. Kamperman, Systematic variation of membrane casting parameters to control the structure of thermo-responsive isoporous membranes, J. Membr. Sci. 548 (2018) 502–509.
- [24] C. Sinturel, F.S. Bates, M.A. Hillmyer, High χ–low N block polymers: how far can we go? ACS Macro Lett. 4 (2015) 1044–1050.
- [25] J.R. Werber, C.O. Osuji, M. Elimelech, Materials for next-generation desalination and water purification membranes, Nat. Rev. Mater. 1 (2016) 16018.
- [26] Y. Wang, W. Xing, N. Xu, Homoporous membranes, Huagong Xuebao/CIESC Journal 67 (1) (2016) 27–40, https://doi.org/10.11949/j.issn.0438-1157. 20151113.
- [27] S.P. Nunes, R. Sougrat, B. Hooghan, D.H. Anjum, A.R. Behzad, L. Zhao, N. Pradeep, I. Pinnau, U. Vainio, K. Peinemann, Ultraporous films with uniform nanochannels by block copolymer micelles assembly, Macromolecules 43 (2010) 8079–8085.
- [28] M. Gallei, S. Rangou, V. Filiz, K. Buhr, S. Bolmer, C. Abetz, V. Abetz, The influence of magnesium acetate on the structure formation of polystyrene-block-poly(4-vinylpyridine)-based integral-asymmetric membranes, Macromol. Chem. Phys. 214 (2013) 1037–1046.
- [29] J.I. Clodt, S. Rangou, A. Schroder, K. Buhr, J. Hahn, A. Jung, V. Filiz, V. Abetz, Carbohydrates as additives for the formation of isoporous PS-b-P4VP diblock copolymer membranes, Macromol. Rapid Commun. 34 (2013) 190–194.
- [30] G. Zhu, Y. Yin, Z. Li, Y. Qiu, Z. Yi, C. Gao, Organic acids interacting with block copolymers have broadened the window that retains isoporous structures, J. Membr. Sci. 582 (2019) 391–401.
- [31] G. Bokias, G. Staikos, I. Iliopoulos, Solution properties and phase behaviour of copolymers of acrylic acid with N-isopropylacrylamide: the importance of the intrachain hydrogen bonding, Polymer 41 (2000) 7399–7405.
- [32] S. Sun, P. Wu, W. Zhang, W. Zhang, X. Zhu, Effect of structural constraint on dynamic self-assembly behavior of PNIPAM-based nonlinear multihydrophilic block copolymers, Soft Matter 9 (2013) 1807–1816.
- [33] G. Zhu, Y. Ying, X. Li, Y. Liu, C. Yang, Z. Yi, C. Gao, Isoporous membranes with sub-10 nm pores prepared from supramolecular interaction facilitated block copolymer assembly and application for protein separation, J. Membr. Sci. 566 (2018) 25–34.
- [34] O. Ikkala, J. Ruokolainen, G.T. Brinke, M. Torkkeli, R. Serimaa, Mesomorphic state of poly(vinylpyridine)-dodecylbenzenesulfonic acid complexes in bulk and in xylene solution, Macromolecules 28 (1995) 7088–7094.
- [35] I. Vukovic, T.P. Voortman, D.H. Merino, G. Portale, P. Hiekkataipale, J. Ruokolainen, G.T. Brinke, K. Loos, Double gyroid network morphology in supramolecular diblock copolymer complexes, Macromolecules 45 (2012) 3503–3512
- [36] K. Mukae, M. Sakurai, S. Sawamura, K. Makino, S.W. Kim, I. Ueda, K. Shirahama, Swelling of poly(N-isopropylacrylamide) gels in water-alcohol (C1-C4) mixed solvents, J. Phys. Chem. 97 (1993) 737–741.
- [37] Y. Xie, B. Sutisna, S.P. Nunes, Membranes prepared by self-assembly and chelation

- assisted phase inversion, Chem. Commun. 53 (2017) 6609-6612.
- [38] C.M. Hansen, Hansen Solubility Parameters : A User's Handbook, second ed., CRC Press, Boca Raton, 2007.
- [39] E. Stefanis, C. Panayiotou, Prediction of Hansen solubility parameters with a new group-contribution method, Int. J. Thermophys. 29 (2008) 568–585.
- [40] N. Hameed, Q. Guo, T. Hanley, Y. Mai, Hydrogen bonding interactions, crystallization, and surface hydrophobicity in nanostructured epoxy/block copolymer blends, J. Polym. Sci. Part B 48 (2010) 790–800.
- [41] N. Lefevre, K.C. Daoulas, M. Muller, J. Gohy, C. Fustin, Self-assembly in thin films of mixtures of block copolymers and homopolymers interacting by hydrogen bonds, Macromolecules 43 (2010) 7734–7743.
- [42] S. Dami, C. Abetz, B. Fischer, M. Radjabian, P. Georgopanos, V. Abetz, A correlation between structural features of an amphiphilic diblock copolymer in solution and the
- structure of the porous surface in an integral asymmetric membrane, Polymer 126 (2017) 376–385.
- [43] S.P. Nunes, A.R. Behzad, B. Hooghan, R. Sougrat, M. Karunakaran, N. Pradeep, U. Vainio, K. Peinemann, Switchable pH-responsive polymeric membranes prepared via block copolymer micelle assembly, ACS Nano 5 (2011) 3516–3522.
- [44] M. Heskins, J.E. Guillet, Solution properties of poly(N-isopropylacrylamide), J. Macromol. Sci., Part A 2 (1968) 1441–1455.
- [45] Y. Hirokawa, T. Tanaka, Volume phase transition in a nonionic gel, J. Chem. Phys. 81 (1984) 6379–6380.
- [46] G.S. Irwan, Y. Aoyama, S. Kuroda, H. Kubota, T. Kondo, Photografting of N-iso-propylacrylamide and glycidyl methacrylate binary monomers on polyethylene film: effect of mixed solvent consisting of water and organic solvent, J. Appl. Polym. Sci. 97 (2005) 2469–2475.